Myxoma virus M-T5 protects infected cells from the stress of cell cycle arrest through its interaction with host cell cullin-1.

Johnston, J; Wang, G; Barrett, J; Nazarian, S; Colwill, K; Moran, M; McFadden, G

Publisher's version / Version de l'éditeur:
https://doi.org/10.1128/JVI.79.16.10750-10763.2005
Journal of Virology, 79, August 16, pp. 10750-10763, 2005

JOURNAL OF VIROLOGY, Aug. 2005, p. 10750–10763 Vol. 79, No. 16
0022-538X/05/$08.00+0 doi:10.1128/JVI.79.16.10750–10763.2005

Myxoma Virus M-T5 Protects Infected Cells from the Stress of Cell Cycle Arrest through Its Interaction with Host Cell Cullin-1

J. B. Johnston,[1]†‡ G. Wang,[1]†‡ J. W. Barrett,[1] S. H. Nazarian,[1,2] K. Colwill,[3]§ M. Moran,[3]¶ and G. McFadden[1,2]*

BioTherapeutics Research Group, Robarts Research Institute, London, Ontario, Canada[1]; Department of Microbiology and Immunology, University of Western Ontario, London, Ontario, Canada[2]; and MDS Proteomics, 251 Attwell Drive, Toronto, Ontario M9W 7H4, Canada[3]

Received 23 March 2005/Accepted 18 May 2005

The myxoma virus (MV) M-T5 gene encodes an ankyrin repeat protein that is important for virus replication in cells from several species. Insight was gained into the molecular mechanisms underlying the role of M-T5 as a host range determinant when the cell cycle regulatory protein cullin-1 (cul-1) was identified as a cellular binding partner of M-T5 and found to colocalize with the protein in both nuclear and cytosolic compartments. Consistent with this interaction, infection with wild-type MV (vMyxlac) or a deletion mutant lacking M-T5 (vMyxT5KO) differentially altered cell cycle progression in a panel of permissive and nonpermissive cells. Cells infected with vMyxlac transitioned rapidly out of the G_0/G_1 phase and preferentially accumulated at the G_2/M checkpoint, whereas infection with vMyxT5KO impeded progression through the cell cycle, resulting in a greater percentage of cells retained at G_0/G_1. Levels of the cul-1 substrate, p27/Kip-1, were selectively increased in cells infected with vMyxT5KO compared to vMyxlac, concurrent with decreased phosphorylation of p27/Kip-1 at Thr187 and decreased ubiquitination. Compared to cells infected with vMyxlac, cell death was increased in vMyxT5KO-infected cells following treatment with diverse stimuli known to induce cell cycle arrest, including infection itself, serum deprivation, and exposure to proteasome inhibitors or double-stranded RNA. Moreover, infection with vMyxlac, but not vMyxT5KO, was sufficient to overcome the G_0/G_1 arrest induced by these stimuli. These findings suggest that M-T5 regulates cell cycle progression at the G_0/G_1 checkpoint, thereby protecting infected cells from diverse innate host antiviral responses normally triggered by G_0/G_1 cell cycle arrest.

The strict dependence of viruses on host cellular metabolic processes for the machinery and precursors necessary to support each unique phase of their life cycle makes the availability of these resources a critical determinant of the outcome of a virus infection. Unlike viruses with smaller genomes and a limited coding capacity for proteins specifically devoted to DNA replication, poxviruses encode the majority of enzymes required for viral genome synthesis (30). This property enables poxviruses to replicate in the cytosol of infected cells independently of the host nuclear machinery, decreasing the dependence of virus replication on the status of the host cell cycle. However, the ability to successfully compete with the host cell for such resources as deoxynucleotides and replicative factors to ensure transcription and translation of viral genes remains a major obstacle that poxviruses must still overcome to efficiently replicate their genomes and generate progeny virions. This requirement necessitates that poxviruses also possess strategies to divert such essential resources and at least transiently create an environment in infected cells that favors virus replication.

Progression through the cell cycle is a highly regulated process during which chromosomes are replicated (S) and then segregated during cytokinesis and mitosis (M) (reviewed in reference 32). These periods of activity are separated by gaps of preparation and dormancy (G_0, G_1, and G_2) that allow for tighter control of cell replication by providing regulatory checkpoints at major transition phases. These checkpoints include G_0/G_1, which regulates the entry of a quiescent cell back into the cycle, G_1/S, which regulates initiation of DNA replication, and G_2/M, which regulates mitosis. This control is largely exerted by the sequential activation of cyclins, which function as the regulatory subunits of the cyclin-dependent kinases (CDKs) to mediate the selective phosphorylation of subsets of regulatory molecules. Because CDKs are constitutively expressed, their activity is regulated positively by the relative abundance of cyclins and negatively by CDK inhibitors (CDK-I), such as p21/waf and p27/Kip. Thus, the key mechanism for controlling progression through the cell cycle is the regulated turnover of cyclins, CDK, and CDK-I through selective synthesis and degradation.

The ubiquitin (Ub)-proteasome system is the primary cellular mechanism for maintaining protein abundance and, as such, is responsible for the selective degradation of regulatory proteins involved in a spectrum of biological functions, including cell cycle progression, apoptosis, and signal transduction (reviewed in references 38 and 39). In this process, termed

* Corresponding author. Mailing address: BioTherapeutics Research Group, Robarts Research Institute, SDRI Rm. 133, 1400 Western Road, London, Ontario N6G 2V4, Canada. Phone: (519) 663-3184. Fax: (519) 663-3715. E-mail: mcfadden@robarts.ca.

† J.B.J. and G.W. contributed equally to this work.

‡ Present address: Institute for Nutrisciences and Health, National Research Council of Canada, Charlottetown, Prince Edward Island C1A 5T1, Canada.

§ Present address: Samuel Lunenfeld Research Institute, Mount Sinai Hospital, Toronto, Ontario M5G 1X5, Canada.

¶ Present address: Hospital for Sick Children, McLaughlin Centre for Molecular Medicine, University of Toronto, Toronto, Ontario M5G 2C1, Canada.

ubiquitination, the concerted activity of a complex of enzymes and support molecules mediates the selective addition of multiple copies of the Ub protein to a target protein and initiates proteolytic attack by the 26S proteasome. These enzymes include an E1 Ub-activating enzyme that activates Ub in an ATP-dependent reaction, an E2 Ub-conjugating enzyme that acts as a shuttle to transfer activated Ub to the target protein, and an E3 Ub-ligating enzyme that catalyzes this transfer reaction. The multisubunit cullin-based E3 ligases, such as cullin-1 (cul-1), are the most extensively studied of the three structural classes of Ub ligases (4). For these ligases, proteins targeted for proteolytic degradation are recognized by a variety of F-box-containing proteins according to specific patterns of phosphorylation. Therefore, the ubiquitination activity of cullins is closely linked to cellular protein phosphorylation networks.

Given the importance of cell cycle in determining not only the availability of resources for viral replication but also the capacity of the host to eliminate infected cells through apoptosis, it is not surprising that numerous viruses have evolved highly specific arsenals of proteins to target the expression and activity of host cell cycle regulators and modulate the intracellular milieu following infection. These strategies typically fall into two functional categories. In the first, viruses force or accelerate entry into the cell cycle to promote the proliferation of host cells and stimulate the synthesis of replicative enzymes and intermediates. For example, the products of the human cytomegalovirus UL68 (18) and adenovirus E1A (33) genes have been shown to stimulate the progression of quiescent cells through G_1 into S phase, a strategy that typically results in the transformation of the infected cells. In the second, viruses impede cell cycle progression and transiently arrest infected cells at specific stages in the cell cycle, which is likely to increase the amount of time spent in a cell cycle phase when the resources required for replicating the virus genome are abundant while impeding transition to a stage at which competing cellular DNA replication machinery is active. This strategy has been reported for both large DNA viruses, such as Kaposi's sarcoma-associated herpesvirus (13) and human herpesvirus 6 (6), which promote arrest at the G_1/S and G_2/M checkpoints, respectively, and small RNA viruses, such as feline immunodeficiency virus (10) and human immunodeficiency virus (16), which induce G_2 arrest. Viruses have also been shown to specifically target and exploit the Ub-proteasome pathway. For example, many viral proteins, such as the human cytomegalovirus UL71 (17) and the human papillomavirus E7 (1) gene products, use this system to promote degradation of the retinoblastoma family of tumor suppressors proteins. Others, such as human papillomavirus E6 (46) and adenovirus E1B 55K/E4orf6 (40) genes, encode proteins that inhibit the activity of the p53 tumor suppressor gene through a similar mechanism. In contrast, the human immunodeficiency virus Tat protein inhibits proteasome function to prevent degradation of viral proteins upon infection (42). Recently, virus-encoded homologs of RING-containing E3 Ub ligases have also been reported in both poxviruses (11, 12, 27, 35) and herpesviruses (5) and shown to possess Ub ligase activity.

The identification of poxviral Ub ligases supports a growing body of evidence suggesting that regulation of the cell cycle is an important factor in the replication of poxvirus. For example, infection of rabbit fibroblasts with the orthopoxvirus vaccinia virus (VV) has been shown to increase transit through G_1 and promote accumulation of cells within the S phase (52). Similar results were obtained when these cells were infected with malignant rabbit fibroma virus (MRV), a chimeric poxvirus encoding sequences from both myxoma virus (MV), a highly virulent leporipoxvirus of rabbits, and Shope fibroma virus (SFV), an avirulent leporipoxvirus (51). Infection with MRV prolonged the G_2/M phase of the cell cycle, resulting in a preferential accumulation of infected cells in G_2/M concurrent with a decrease in the number of cells in the G_0/G_1 phase. Of interest, the avirulent SFV did not significantly alter cell cycle progression following infection, while the effect of infection with MV was not assessed (51).

Although MV exhibits strict species specificity for the rabbit and is nonpathogenic in other vertebrates, growing evidence indicates that the virus can productively infect cells from diverse species in vitro (14, 15, 45, 53). One determinant implicated in the MV host range is the product of the M-T5 gene, an ankyrin (ANK) repeat-containing protein that has been shown to be critical for replication in both rabbit lymphocytes and many human tumor cell lines (31, 45). Despite its obvious importance to MV pathogenesis, a molecular basis for the function of M-T5 and its role in MV tropism remains unclear. However, several properties of M-T5 suggest that it may play a role in manipulating the cell cycle following MV infection. For example, deletion of M-T5 has been shown to result in an abortive infection of rabbit lymphocytes due to a shut-down of host and viral protein synthesis that culminates in apoptosis, a consequence typical of lymphocytes undergoing cell cycle arrest (31). Moreover, the ANK repeat is a protein interaction domain first identified in yeast cell cycle regulators and subsequently shown to be a feature of many other proteins involved in regulation of the cell cycle and proteasome activity (29, 41). Finally, we show here that M-T5 contains a putative C-terminal F-box-like domain, the target recognition sequence associated with F-box proteins of cullin-based E3 ligase complexes (7).

Consistent with these properties, we report that M-T5 is required for MV-infected cells to overcome the cell cycle arrest induced by infection and other stress stimuli, thereby protecting cells from diverse cell death pathways. This function reflects a direct physical interaction between M-T5 and the cellular E3 Ub ligase, cul-1, that promotes increased ubiquitination and proteasomal degradation of cell cycle regulators, such as the CDK-I p27/Kip. Thus, M-T5 represents a poxvirus-encoded cell cycle regulatory protein that is capable of manipulating the Ub-proteasome degradation of cell cycle control proteins in infected cells.

MATERIALS AND METHODS

Cell culture. Baby green monkey kidney (BGMK) cells, African green monkey kidney cells (COS-7), and the human tumor cell lines 786-0, Caki-1, and MCF-7 (NCI-60 reference collection) were propagated in Dulbecco's modified Eagle medium completed with 10% fetal bovine serum (Sigma, Oakville, Canada), 100 U penicillin/ml, and 100 μg streptomycin/ml (Invitrogen, Burlington, Canada). HEK293 epithelial cells (a gift of Y. Ma, Kyoto University) were grown in complete RPMI 1640 medium. Primary human dermal fibroblasts were derived from explant cultures of neonatal foreskin tissue as described previously (15) and grown in complete Dulbecco's modified Eagle's medium. For cell cycle synchro-

nization, cells were incubated in the appropriate medium in the absence of serum for 36 to 48 h prior to use.

Viruses and infections. Two recombinant MVs (strain Lausanne) expressing a β-galactosidase cassette driven by the MV late gene promoter were used for infection studies: vMyxlac, a control virus expressing wild-type M-T5, and vMyxT5KO, which fails to express M-T5 due to targeted disruption of both copies of the M-T5 open reading frame (ORF) (M005R/L) (31). Both viruses were propagated and titrated by focus formation on BGMK cells as described previously (36). For infection, cells were incubated with the indicated multiplicity of infection (MOI) of either virus for 1 h at 37°C, after which infected cells were washed to remove excess virus and cultured in normal medium until used in subsequent experiments. For β-galactosidase expression studies, cells infected with vMyxlac were washed with phosphate-buffered saline (PBS) at various time points postinfection, fixed for 5 min in neutral buffered formalin (PBS and 3.7% formaldehyde), and incubated for 4 h at 37°C with 5-bromo-4-chloro-3-indolyl-β-D-galactopyranoside (X-Gal) staining solution (100 μg/ml X-Gal, 500 μM potassium ferrocyanide and ferrocyanide, and 200 μM $MgCl_2$ in PBS). For genes expressed in a pSC65 plasmid background, and thus driven by a synthetic early-late VV promoter, cells were infected with VV (strain Copenhagen) at an MOI of 5 prior to transfection.

Generation of polyclonal anti-M-T5 antiserum. A peptide (Fig. 1C) beginning at amino acid (aa) 430 of M-T5 was chosen and synthesized (Invitrogen) based on its antigenic profile. The peptide was conjugated to keyhole limpet hemocyanin using the Imject Immunogen EDC conjugation kit (Pierce, Rockford, IL) according to the manufacturer's instructions. The peptide-keyhole limpet hemocyanin conjugate was suspended in Freund's complete adjuvant (Sigma) for the initial injection into a New Zealand White rabbit. Four subsequent injections were performed to boost antibody titers in Freund's incomplete adjuvant (Sigma). Antibody titer was assessed following immunoblotting of myxoma virus infection of BGMK cell lysates. The antiserum was purified on an affinity purification column against M-T5 peptide conjugated to bovine serum albumin using the Aminolink Plus immobilization kit (Pierce) following the manufacturer's protocol.

Fusion proteins, epitope-specific antibodies, and reagents. The M-T5 ORF was PCR amplified from viral genomic DNA and cloned into appropriate expression vectors using restriction sites introduced by the PCR primers. Constructs included fusion proteins expressing tandem affinity purification tag (TAP; pcDNA3.6-TAP), Myc (pcDNA3.1-Myc-His; Invitrogen), enhanced green fluorescent protein (EGFP; pEGFP-C1; Clontech, Mississauga, Canada), Flag (pCMV-Flag; Sigma), hemagglutinin (HA; pcDNA3-HA), or T7 (pcDNA3-T7) epitopes (summarized in Fig. 1A). M-T5 expressing the TAP epitope was subsequently subcloned into the pSC65 vector. Plasmids encoding human cul-1 tagged with HA (pcDNA3-HA-CUL1) or Flag (pcDNA3-Flag-CUL1) epitopes were kindly provided by Y. Xiong (University of North Carolina) and Z. Q. Pan (Mount Sinai School of Medicine, New York, N.Y.), respectively. Vector encoding myc-tagged human Ub (pcDNA3.1Myc-Ub) and the pcDNA3-HA plasmid were provided by J. Q. Cheng (Moffitt Cancer Center and Research Institute, Florida). TAP-tagged and red fluorescent protein (RFP)-tagged constructs were subsequently generated by subcloning cul-1 into pcDNA3.6-TAP and pDsRed2-C1 (Clontech) vectors, respectively. The identities of all clones were confirmed by sequence analysis, and expression of fusion proteins was confirmed by fluorescence microscopy or Western analyses using mouse monoclonal antibodies specific for Myc (Invitrogen), T7 (Novagen, San Diego, CA), Flag (Sigma), or HA (Roche, Mississauga, Canada) epitopes. Gel shift analysis was used to confirm that the fluorescence observed represented a GFP fusion product. A rabbit peroxidase-antiperoxidase antiserum (anti-PAP; Sigma) recognizing the protein A sequence was utilized for detecting the TAP tag.

Stable expression of M-T5 in HEK293 cells. Control pcDNA3 plasmid and the pcDNA3T7-MT5 construct were transiently transfected into HEK293 cells by using Lipofectamine 2000 reagent (Invitrogen) according to the manufacturer's protocols. Transfected cells were subjected to Geneticin selection (G418; 1,000 μg/ml; Invitrogen) over several weeks to identify putative stable transfectants and amplified in complete RPMI 1640 supplemented with 500 μg of G418/ml. Reverse transcription-PCR and immunoblot analysis verified the incorporation and expression by stable clones of either T7-tagged M-T5 (HEKT7MT5) or the control neomycin resistance gene (HEKneo).

Subcellular localization of M-T5. HEKT7MT5 cells that stably expressed T7-tagged M-T5 were adhered to poly-L-lysine-coated glass coverslips and grown to 70% confluence. T7 M-T5 expression was detected by indirect immunofluorescence using monoclonal antibody specific for the T7 epitope (1:100 dilution) and a fluorescein isothiocyanate-conjugated goat anti-mouse secondary antibody (1:500 dilution; Jackson ImmunoResearch, West Grove, PA). Isotype control antibodies were used with transfected and nontransfected cells to control for nonspecific antibody binding. Cytosolic or nuclear localization was assessed by counterstaining with fluorescent markers (Molecular Probes, Eugene, OR) specific for actin (Texas Red-X phalloidin; 1:20) or nuclei (4′,6′-diamidino-2-phenylindole [DAPI]; 1:330). To investigate colocalization with cul-1, COS-7 cells were adhered to coverslips, grown to 90% confluence, and transfected with plasmids encoding M-T5 fused to GFP- and RFP-tagged cul-1 using Lipofectamine 2000 reagent. Untransfected cells and cells transfected with the appropriate plasmid lacking exogenous sequences (vector alone) served as controls for both cell types. At 36 h posttransfection, cells were mounted in Prolong Antifade medium (Molecular Probes) and examined under a Leica fluorescence microscope using the appropriate filter.

Cell cycle analysis. Cells were harvested by trypsinization, washed twice with PBS, and pelleted by centrifugation at 500 ×*g* for 5 min. Washed cells were suspended in 1 ml of cold absolute methanol added dropwise while vortexing to prevent cell clumping and fixed by incubation for a minimum of 6 hours at 4°C. Fixed cells were pelleted by centrifugation to remove the methanol, washed twice with PBS, and incubated covered at room temperature for 30 min in 0.5 ml of PBS containing 50 μg propidium iodide (PI)/ml (Sigma) and 50 μg RNase A/ml (Sigma). Debris and doublets were eliminated from the analyses using pulse width/area discrimination. Following flow cytometry, data analysis was performed using the ModFitLT software (Verity Software, Topsham, ME).

Immunoblot analysis. Cultured cells were lysed in buffer containing 10 mM Tris, pH 4.0, 10 mM NaCl, 3 mM $MgCl_2$, and 0.5% Tween 20, sonicated to solubilize proteins, and cleared by centrifugation. Protein levels were quantified using a protein assay kit (Bio-Rad, Mississauga, Canada), and 25 μg of each sample was separated by sodium dodecyl sulfate-polyacrylamide gel electrophoresis (SDS-PAGE). Separated proteins were transferred to nitrocellulose and blocked with 5% skim milk in TBST (25 mM Tris-buffered saline and 0.5% Tween 20). Primary antibodies were diluted in 5% milk–TBST and incubated with membranes for 1 h at room temperature. Membranes were washed and incubated for 1 h at room temperature with horseradish peroxidase-conjugated secondary antibodies diluted 1:3,000 in 5% milk–TBST. Immunoreactive proteins were detected by chemiluminescence (Perkin-Elmer, Boston, MA). Loading of equal amounts of protein from each sample was confirmed by detection of the housekeeping gene actin. Polyclonal antibodies used included those specific for human cul-1 (NeoMarker, Fremont, CA), unphosphorylated (C-19, Santa Cruz Biotechnology, Santa Cruz, CA) and Thr187-phosphorylated (Upstate Biotechnology, Lake Placid, NY) p27/Kip1, caspase-3 (Cell Signaling Technology, Beverley, MA), and actin (Santa Cruz Biotechnology). Monoclonal antibodies used included those detecting poly(ADP-ribose) polymerase (PARP; 4C10-5; BD Pharmingen, Mississauga, Canada) and Ub. Horseradish peroxidase-conjugated goat-anti-mouse and goat-anti-rabbit secondary antibodies were obtained from Jackson ImmunoResearch Laboratories.

Identification of M-T5 interacting proteins. M-T5 interacting proteins were identified using immunoblotting, TAP, and mass spectrometry analyses as described previously (54). Briefly, T7- or TAP-tagged host and viral proteins were expressed in HEK293 cells by calcium phosphate transfection in accordance with the manufacturer's protocols (Clontech). For T7 fusion proteins, lysates were harvested after 48 h and incubated overnight with protein A/G-agarose beads (Upstate Biotechnology) conjugated with anti-T7 antibody. Beads were pelleted by centrifugation and washed twice, and the immunocomplexes were resolved by SDS-PAGE. For TAP fusion proteins, cells were lysed in 2% 3-[(3-cholamidopropyl)-dimethylammonio]-1-propanesulfonate buffer containing protease inhibitors and cleared lysates incubated with rabbit immunoglobulin G agarose beads (Sigma) for 2 h at 4°C. Beads were washed three times, and bound protein was released using the TAP method described previously (54). Immunoblot analyses were performed as described above using the appropriate antibodies. For mass spectrometry analyses, proteins separated by SDS-PAGE were visualized using Gel-Code Blue (Pierce) or silver (Bio-Rad) stains. Bands present in cells transfected with plasmid encoding M-T5, but not in lysates from control samples transfected with empty vector, were cut from the gel and subjected to in-gel digestion. The identity of the proteins comprising each band was determined by matrix-assisted laser desorption ionization–time-of-flight mass spectrometry.

Ubiquitination assay. Human 786-0 tumor cells were seeded in 10-cm dishes at 50% confluence and incubated in the absence of serum for 48 h to synchronize the cell cycle. Synchronized cells were initially transfected with plasmid encoding Myc-tagged Ub using Lipofectamine 2000 reagent, incubated for 24 h, and then infected with vMyxlac or vMyxT5KO (MOI = 5). At 12 h postinfection (hpi), cells were incubated with the proteasome inhibitor *N*-acetyl-Leu-Leu-Norleu-al (LLnL; Sigma) at a concentration of 50 μM for 5 h. Cells were harvested, and p27/Kip-1was immunoprecipitated from cell lysates using the anti-p27 antibody conjugated to protein A-agarose beads. Polyubiquinated p27 was detected by immunoblotting using antibodies specific for either the Myc epitope or Ub itself.

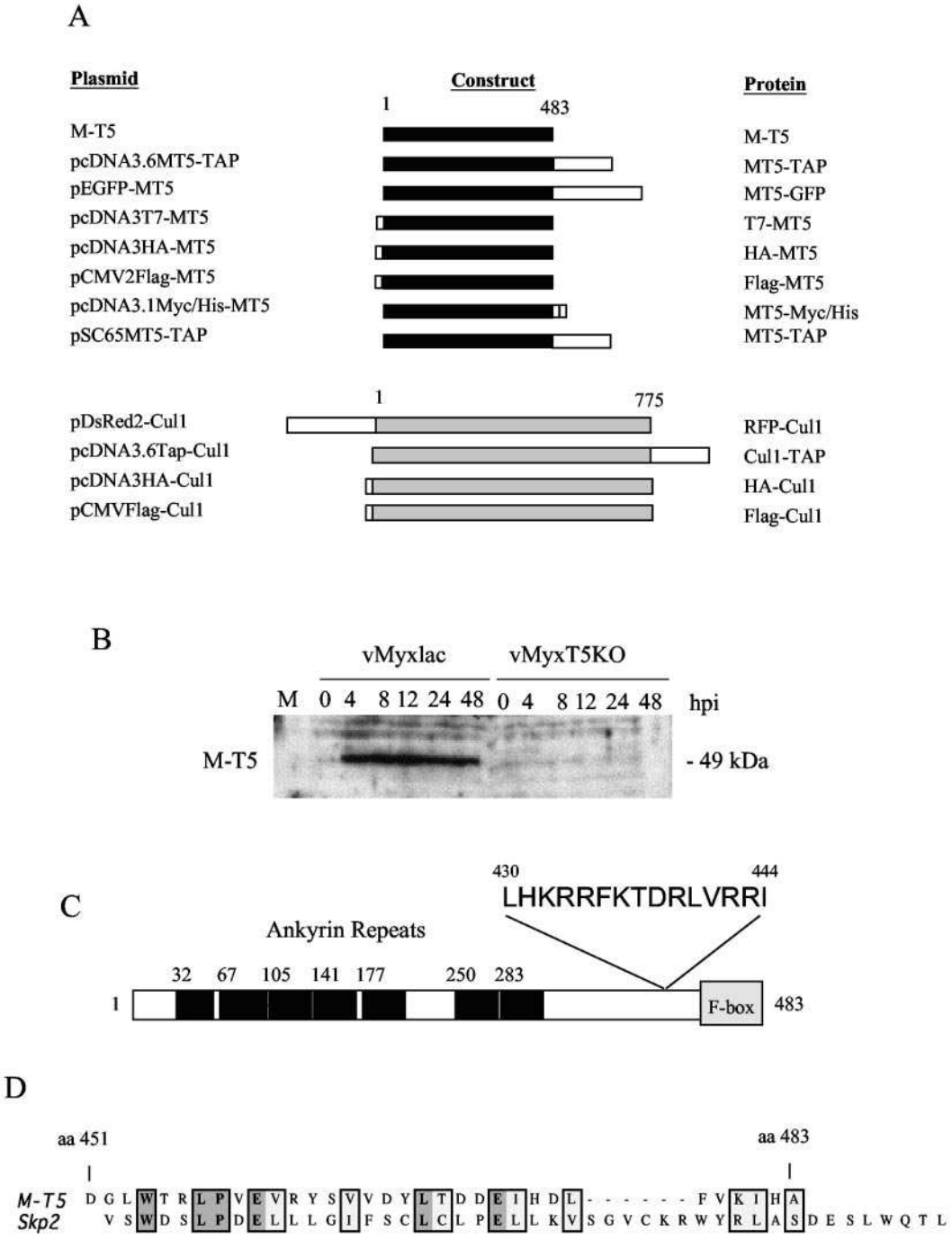

FIG. 1. Properties of M-T5 and summary of the M-T5 and cul-1 constructs employed in this study. A. MV M-T5 and human cul-1 were either left untagged or fused to TAP, GFP, T7 epitope, HA, Flag, Myc, or RFP tags. The TAP epitope consists of the protein A immunoglobulin G binding sequence and the calmodulin binding protein domain separated by a tobacco etch virus protease cleavage site. B. Immunoblot analysis of lysates from human 786-0 tumor cells collected between 4 and 48 hpi with wild-type virus (vMyxlac) or the M-T5 deletion mutant (vMyxT5KO) at an MOI of 5. The 49-kDa band corresponding to M-T5 is indicated. C. Schematic representation of the 483-aa M-T5 ORF, indicating the seven putative ANK repeat domains (black boxes) and the C-terminal F-box-like motif (gray box). Indicated are the first residues of each predicted ANK repeat. The sequence starting at aa 430 indicates the peptide used to create anti-M-T5 polyclonal antibody. D. Alignment of the C-terminal region of M-T5 (aa 451 to 483) and the F-box motif of Skp2. Identical and similar residues are indicated by dark and light shading, respectively.

Cytotoxicity and apoptosis assays. Stimuli included infection with vMyxlac or vMyxT5KO at the indicated MOI, serum deprivation, and treatment with either the proteasome inhibitor LLnL (10 μM), the proapoptotic agent staurosporine (50 nM), or poly(I:C) double-stranded RNA (dsRNA; 20 μg/ml). Cell viability and apoptosis were assessed at various time points posttreatment by immunoblot detection of caspase-3 activation and PARP cleavage or by using the assays described below. To inhibit caspase activity, cells were treated with the pan-caspase inhibitor Z-VAD-FMK (Sigma) at a concentration of 60 μM.

Trypan blue exclusion. Cells were washed twice with PBS and incubated at room temperature for 15 min in a 0.2% solution of trypan blue dye (Sigma) in PBS. Cells were washed again with PBS, and the percentage of viable cells was calculated as the number of cells that remained impermeable to the dye divided by the total number of cells.

Annexin V staining. Duplicate aliquots of 1×10^5 cells were washed three times in PBS and resuspended in 100 μl of binding buffer (10 mM HEPES-NaOH, 140 mM NaCl, 2.5 mM $CaCl_2$). To each sample, 5 μl of fluorescein isothiocyanate-conjugated Annexin V (Pharmingen) and 2 μl of PI were added, followed by incubation at room temperature for 15 min. To control for nonspecific binding, cell aliquots were incubated with Annexin V or PI alone, while cells resuspended in binding buffer alone served as negative controls. Stained cells were immediately analyzed by flow cytometry using a FACSCalibur apparatus and CellQuest software (Becton Dickinson).

Terminal deoxynucleotidyltransferase-mediated dUTP-biotin nick end labeling (TUNEL) assay. DNA fragmentation was assessed using a colorimetric terminal deoxynucleotidyl transferase-FragEl DNA fragmentation assay (Calbiochem) according to the manufacturer's protocols. Apoptotic nuclei were visualized following incubation with 3′,3′-diaminobenzidine in hydrogen peroxidase-urea and methyl green counterstaining and mounted on glass slides for analysis by light microscopy. Apoptotic cells were distinguished by the presence of nuclei that were stained a deep brown, while nonapoptotic nuclei were stained blue-green. The number of 3′,3′-diaminobenzidine-stained cells in six fields was counted and expressed relative to the total number of cells in each field.

Lysosomal staining. Cells were incubated for 30 min at 37°C with LysoTracker Red DND-99 (Molecular Probes), a fluorescent stain specific for lysosomes, diluted 1:13,000 in prewarmed complete medium. Lysosomal staining was assessed by flow cytometry.

RESULTS

Structural motifs of the M-T5 protein. Previous reports from our laboratory demonstrated that the MV M-T5 gene product is a virulence factor that is a critical determinant of cell tropism in both rabbit lymphocytes (31) and human cancer cells (45). This phenotype has been shown to be associated with an abortive infection of rabbit lymphocytes and restricted spread within diverse human tumor cell lines. The M-T5 gene is present in two copies within the terminal inverted repeats regions of the MV genome and encodes a 49-kDa, nonsecreted, early virus protein (2, 31). To study the expression of M-T5, we have constructed a variety of tagged versions of M-T5 (Fig. 1A) and created an antipeptide polyclonal antibody to M-T5 (see Materials and Methods). Using the anti-M-T5 antibody, we were able to show that M-T5 is expressed rapidly following infection of both rabbit cells (not shown) and the 786-0 human tumor cell line (Fig. 1B). M-T5 remains as an abundant and stable 49-kDa cell-associated protein throughout the course of infection and is absent from cells infected with vMyxT5KO (Fig. 1B). Earlier studies reported that M-T5 does not possess significant sequence similarity with any nonviral protein but does exhibit a low level of similarity with several other poxvirus proteins known to be determinants of host range (31). Despite the absence of obvious similarity to cellular proteins of known function, more detailed analyses of the M-T5 protein sequence do reveal the presence of several conserved motifs. Most evident, M-T5 is predicted to encode seven ANK repeat domains within the N-terminal and central regions of the protein (Fig. 1C). Due to the relatively ubiquitous nature of the ANK repeat, however, this finding in itself provides little insight into the potential function of M-T5. Of greater interest, M-T5 also possesses a C-terminal domain that closely resembles the F-box-like motif (Fig. 1C). The F-box domain is a protein-protein interaction motif commonly found in proteins, such as Skp2, that function as the recognition subunits of Ub ligase complexes (4). Moreover, the C terminus of M-T5 aligns with the F-box of Skp2 at residues critical for function (Fig. 1D). Thus, we investigated potential interactions between M-T5 and regulatory elements within this pathway.

M-T5 interacts with cul-1. To investigate a molecular basis for these observations and better characterize the function of M-T5, we attempted to identify cellular binding partners for the protein. Preliminary coimmunoprecipitations of 293T cells transfected with pCMV2 Flag-MT5 revealed a variety of potential host binding partners for MT5, under the same conditions used to identify the interaction between myxoma virus M11L and host Bak (54). In this initial screen, the proteins that copurified with Flag-tagged M-T5 protein included DNA-PK, EF1a, and cul-1 (data not shown), but with this protocol considerable variation occurred between various runs. Accordingly, other tagged revisions of M-T5 were also explored. Transient expression of T7 epitope-tagged M-T5 in HEK293 cells followed by immunoprecipitation using anti-T7 antibody revealed a major protein species of approximately 86 kDa that coimmunoprecipitated with M-T5 (Fig. 2A). Immunoblotting with anti-cul-1 identified this protein as human cul-1, a mammalian E3 Ub ligase and regulator of the cell cycle at the G_0/G_1 checkpoint (7). To confirm the specific interaction between M-T5 and cul-1, TAP-tagged M-T5 was expressed in HEK293 cells and binding partners were assessed by TAP isolation and Western blotting. As shown in Fig. 2B, cul-1 was again found to copurify with M-T5, either when the viral protein was overexpressed by transient transfection or when M-T5 was expressed in the context of a poxvirus infection. This finding was supported by the reciprocal experiment in which T7-tagged M-T5 was detected by Western blotting in eluants following TAP isolations using cul-1 as the bait (Fig. 2C). Finally, the interaction between M-T5 and cul-1 was assessed under conditions using HEK293 cells stably transfected with T7-tagged M-T5. Following pull-downs using the anti-T7 epitope antibody, cul-1 was detectable in eluants from the stable HEKT7MT5 cells but not from the control cell line expressing the neomycin cassette alone (Fig. 2D).

Based on the lack of traditional signal sequences for either secretion or nuclear localization, M-T5 was predicted to be a cytosolic protein (2). However, indirect immunofluorescence to detect expression of T7-tagged M-T5 in uninfected HEKT7MT5 cells revealed that M-T5 was abundantly expressed in the nucleus, colocalizing with the DNA stain DAPI, but not with a fluorescent marker specific for cytosolic actin (Fig. 3A to F). Consistent with the identification of cul-1 as a binding partner of M-T5, albeit not definitive evidence of a functional interaction, both proteins were found to largely colocalize within the nucleus of transfected COS-7 cells with low levels of expression in the cytosol (Fig. 3G to I). Of note, M-T5 has been found to localize to both virus factories and nuclei in vMyxlac-infected cells, but a similar localization of cul-1 to virus factories has not been observed (data not shown). Taken together, these findings demonstrated that M-T5 interacted with human cul-1 under diverse experimental conditions. Moreover, both proteins colocalized within the nucleus of uninfected cells that stably express M-T5 despite the absence of any obvious nuclear localization sequence within the M-T5 protein.

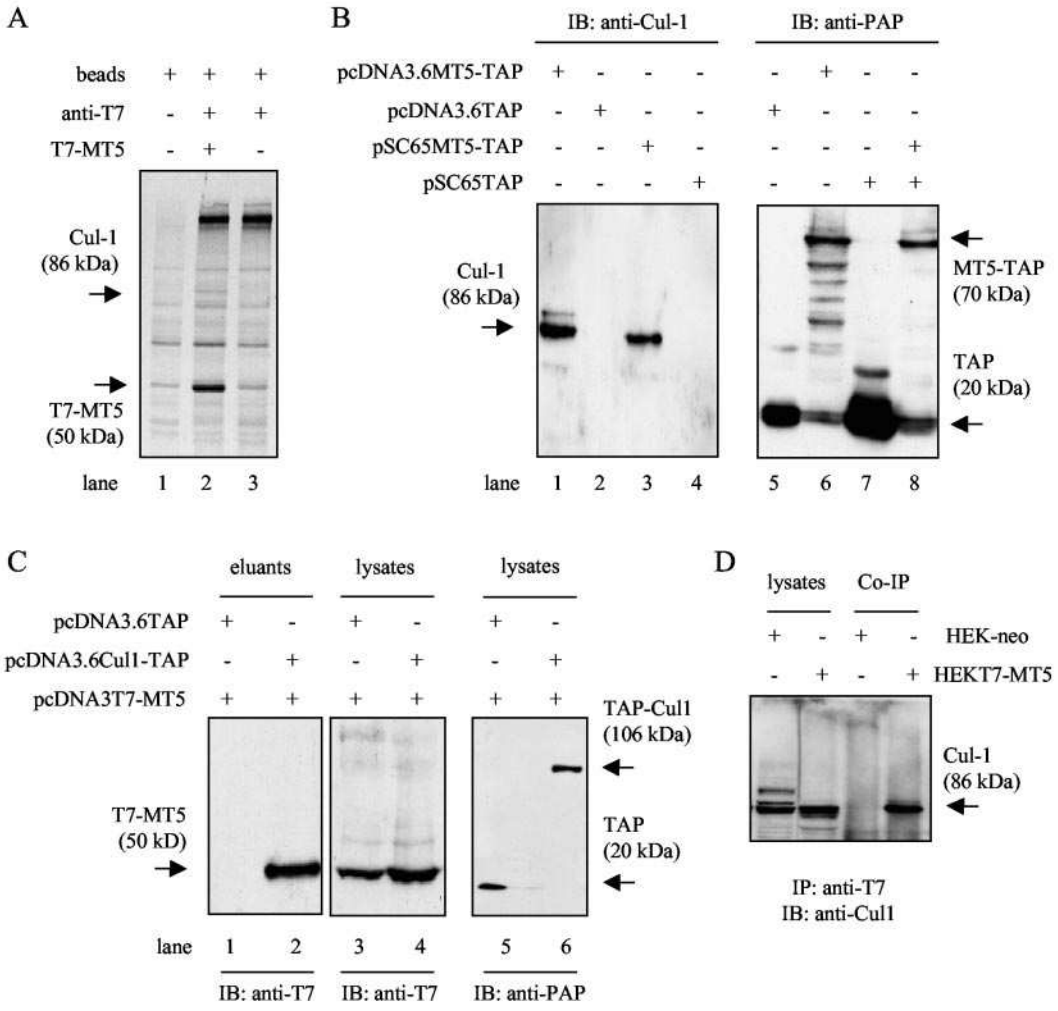

FIG. 2. Identification of human cul-1 as a binding partner of M-T5. A. T7-tagged M-T5 was transiently expressed in HEK293 cells, and cul-1 was identified as a binding partner by mass spectrometry following immunoprecipitation with antibody against the T7 epitope (anti-T7). Immunoprecipitations performed with beads alone (lane 1) and with lysates from mock-transfected cells (lanes 3) served as controls. A representative silver-stained gel is shown. B. TAP-tagged M-T5 was overexpressed in HEK293 cells by transfection using the pcDNA3.6 vector (lanes 1, 2, 5, and 6) or by transfection using the pSC65 vector and infection with vaccinia virus (lanes 3, 4, 7, and 8). cul-1 was detected in eluants from cells transfected with vector encoding M-T5 (lanes 1 and 3) by immunoblotting (IB) with antibody specific for cul-1 (anti-Cul-1), but not in controls transfected with empty vector (lanes 2 and 4). Expression of M-T5 was confirmed by immunoblotting with antibody against the TAP epitope (anti-PAP) in cells transfected with vector encoding the protein (lanes 6 and 8), but not in controls transfected with empty vector (lanes 5 and 7). C. TAP-tagged cul-1 and T7-tagged M-T5 were coexpressed in HEK293 cells, and their interaction was assessed following TAP isolation of cul-1 and detection of M-T5 in eluants (lanes 1 and 2) by immunoblotting. Cells transfected with vector expressing the TAP epitope alone served as controls (lanes 1, 3, and 5). Expression of M-T5 (lanes 3 and 4) and cul-1 (lanes 5 and 6) in cell lysates was confirmed by immunoblotting with antibody against their respective tags. D. HEK293 cells were stably transfected with plasmid encoding T7-tagged M-T5 (HEK-MT5) or the control neomycin cassette (HEK-neo), and the interaction between M-T5 and cul-1 was assessed by coimmunoprecipitation using the antibody against the T7 epitope and immunoblotting with antibody against cul-1.

M-T5 promotes the transition of infected cells out of G_0. We next assessed whether the observed interaction between M-T5 and cul-1 had biological consequences by using a panel of cells previously shown to differ in their permissiveness to infection by wild-type MV and the M-T5 knockout (KO) virus, vMyxT5KO (45). Given the role of cul-1 in cell cycle regulation, these experiments initially focused on the impact of M-T5 expression on the ability of cells to progress through the cell cycle following synchronization in the G_0/G_1 phase by serum deprivation. Representative cell lines permissive to both viruses (BGMK), permissive to wild-type but not M-T5 KO virus (786-0), or nonpermissive to both viruses (MCF7) are shown. Compared to mock-infected cells, increased transition out of the G_0/G_1 arrest induced by serum deprivation was observed following vMyxlac infection of permissive BGMK and 786-0 cells, but not of nonpermissive MCF-7 cells (Fig. 4A). This induction manifested as a 126.4% (BGMK) and 82.7% (786-0) increase in the ratio of cells in the S and G_2/M phases compared to controls. This effect was not observed following infection by vMyxT5KO. The progression of both permissive BGMK cells and nonpermissive MCF-7 cells out of G_0/G_1 was not significantly altered compared to mock-infected cells fol-

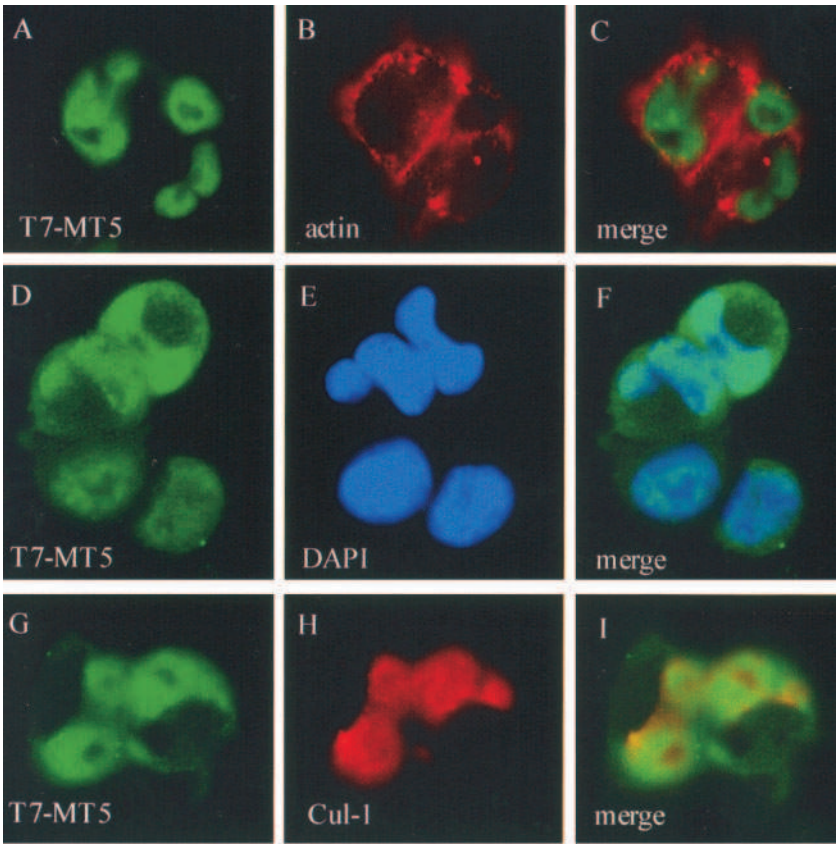

FIG. 3. M-T5 and cul-1 colocalize within the nucleus. The subcellular localization of M-T5 was assessed in HEK293 cells stably transfected with T7-tagged M-T5. M-T5 (A, D, and G) and cul-1 (H) were detected by indirect immunofluorescence using GFP- and RFP-conjugated secondary antibodies, respectively. Actin was detected using Texas Red-X phalloidin (B), and nuclei were detected using DAPI reagent (E). Merged fields are shown in panels C, F, and I.

lowing infection with the KO virus (Fig. 4A). Moreover, infection of nonpermissive 786-0 cells was associated with an abortive phenotype, as indicated by a leftward shift of the histogram and the accumulation of smaller particulate bodies, suggesting loss of cell integrity in these cultures (Fig. 4A).

Previous studies have suggested a link between the virulence of leporipoxviruses and their ability to influence the host cell cycle upon infection (51). Specifically, cells infected with the highly pathogenic MRV, but not avirulent SFV, were found to accumulate preferentially within the S and G_2/M phases of the cell cycle. Since MRV is a chimera of both SFV and MV, we assessed the impact of MV infection on cell cycle progression. As reported for MRV, we observed a progressive increase in the number of cells in G_2/M following infection of BGMK cells with vMyxlac and an increased propensity for cells to accumulate in this phase compared to the typical progression through the cell cycle exhibited by mock-infected cells (Fig. 4B). In contrast, cells infected with vMyxT5KO accumulated within the G_0/G_1 fraction, with consistently fewer cells detected in the S and G_2/M phases over the time course compared to wild-type-infected cultures (Fig. 4B). It is unlikely that these changes in PI staining simply reflected virus replication and subsequent detection of virus genomes. As shown in Fig. 4A and B, changes in PI incorporation indicative of progression through the cell cycle were observed following infection of BGMK cells with vMyxlac, but not vMyxT5KO, despite the fact that both viruses have been shown to replicate at comparable levels in these cells (45).

These results suggested that M-T5 contributed to the ability of infected cells to progress out of the G_1/G_0 checkpoint, a finding consistent with its ability to interact with cul-1. To determine if expression of M-T5 was itself sufficient to overcome persistent growth arrest, BGMK cells were synchronized in the G_0/G_1 phase by serum deprivation and infected with either wild-type or KO virus in the continued absence of serum. BGMK cells were selected for these experiments because they are more resistant to the cytotoxic effects of serum deprivation than 786-0 tumor cells. Sustained serum deprivation induced excessive amounts of cell death in 786-0 cells that precluded accurate assessment of the effects of M-T5 (data not shown). Despite the absence of serum, cells infected with vMyxlac rapidly progressed out of G_0/G_1 and began to accumulate in S and G_2/M phases (Fig. 4C). In contrast, cells infected with vMyxT5KO exhibited little ability to overcome the growth arrest and, in fact, extensive cytotoxicity was evident in these cultures (Fig. 4C). Because cell death was not evident in BGMK cells infected with the M-T5 KO virus in the absence of serum deprivation, these observations suggested that M-T5 expression was required to overcome the cell cycle arrest induced by the lack of serum. This hypothesis was fur-

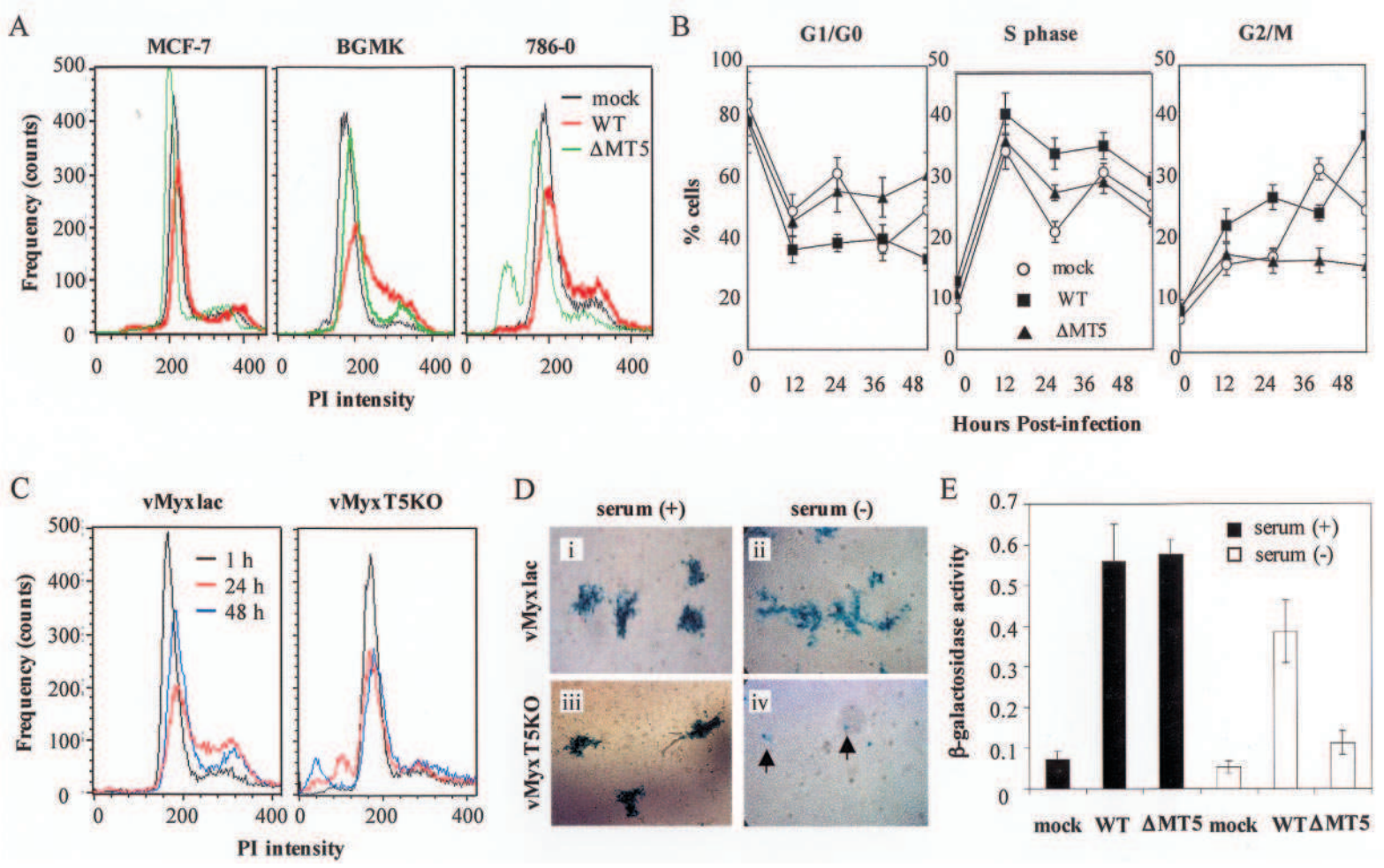

FIG. 4. Expression of M-T5 alters the progression of cells through the cell cycle. A. MCF-7, BGMK, and 786-0 cells were synchronized by serum deprivation for 36 h and then mock infected or infected with vMyxlac (WT) or vMyxT5KO (ΔMT5) at an MOI of 3. Cells were cultured in medium containing serum, and cell cycle progression was assessed at 6 hpi by PI staining and flow cytometry. Representative histograms are shown for each cell line, indicating the G_1/S and G_2/M phases at intensities of 200 and 400 units, respectively. B. BGMK cells were synchronized and infected as described for panel A, and the number of cells in each phase of the cell cycle was assessed by flow cytometry at the indicated time points postinfection. Values represent the mean ± standard deviation (SD) of triplicate samples. C to E. BGMK cells were synchronized by serum deprivation, infected with vMyxlac or vMyxT5KO at an MOI of 3, and cultured for 48 h in the absence of serum. Progression through the cell cycle was determined by PI staining and flow cytometry analysis (C). Replication in synchronized BGMK cells that were cultured in the presence (serum +) or absence (serum -) of serum for 48 h after infection with wild-type or KO virus was assessed by β-galactosidase staining of the characteristic foci formed by MV (D) and quantified by a chromogenic assay to measure β-galactosidase activity (E). Representative images are shown demonstrating foci formation by vMyxlac regardless of serum conditions (i and ii) and by vMyxT5KO when serum was present (iii). Individual cells infected with vMyxT5KO are evident under conditions of serum deprivation (iv, arrows). Values shown from the chromogenic assay (E) represent mean activity (± SD) obtained from triplicate experiments.

ther supported by the finding that serum deprivation also impacted on the ability of each virus to replicate in BGMK cells. Infection with either vMyxlac or vMyxT5KO in the presence of serum was fully productive, as evidenced by typical foci formation (Fig. 4D) and abundant β-galactosidase expression (Fig. 3E). Although foci formation and gene expression were still evident in vMyxlac-infected BGMK cells in the absence of serum, vMyxT5KO was unable to replicate and spread in these cells under conditions of serum deprivation (Fig. 4D and E). Taken together, these findings suggested that M-T5 functioned as a virus-encoded cell cycle regulator capable of overcoming induced growth arrest at the G_0/G_1 checkpoint. Moreover, this property was closely linked to the capacity of MV to productively infect permissive cell lines in the face of stress stimuli like serum deprivation.

M-T5 promotes the phosphorylation, ubiquitination, and degradation of p27 in infected cells. Regulation by *cul-1* of the cell cycle at the G_0/G_1 checkpoint involves control of the expression and activity of p27/Kip1 (34). In this process, transition through G_0/G_1 requires ubiquitination of p27 by cul-1 and subsequent degradation through the 26S proteasome pathway (34). To determine if the apparent cell cycle effects associated with M-T5 expression involved regulation of p27 function, human 786-0 cells were infected with wild-type or KO virus and p27 levels were assessed at various time points postinfection by Western blotting. Although p27 levels were not significantly affected following infection with vMyxlac, p27 accumulation was evident by 8 hpi in cells infected with vMyxT5KO (Fig. 5A, upper lanes). Consistent with these changes, phosphorylation of p27 at Thr187, a prerequisite for recognition by cul-1, was abundant in 786-0 cells infected with wild-type virus but absent in KO virus-infected cells (Fig. 5A, middle lanes). Moreover, immunoprecipitation assays revealed that the accumulation of p27 in vMyxT5KO-infected cells correlated with decreased ubiquitination of the protein (Fig. 5B, lanes 1 to 3). Compared to vMyxlac-infected cells, in which polyubiquinated forms of p27 were evident as a continuous smear (Fig. 5B, lane 2), ubiqinated p27 was detectable in KO virus-infected cultures (Fig. 5B, lane 3) at levels more comparable to mock-infected cells (Fig. 5B, lane 1) despite the fact that p27 protein was more abundant (Fig. 5B, lanes 4 to 6). Thus, deletion of M-T5 was associated with the excessive accumulation of p27 protein due to decreased ubiquitination and proteasome-mediated degradation.

Infection of nonpermissive cells with M-T5 KO virus results in both apoptotic and nonapoptotic cell death. Virus infection initiates a cascade of events that can culminate in cell cycle arrest and the ultimate destruction of infected cells by apoptosis. Moreover, accumulation of p27, as was observed in vMyxT5KO-infected cells, is itself a proapoptotic stimulus that has been shown to induce G_1 arrest and apoptosis in a variety of tumor cell lines, including 786-0 cells (20, 21, 25, 28, 55), providing a potential explanation for the abortive infection associated with M-T5 knockout virus infection. To investigate this possibility, BGMK and 786-0 cells were infected with vMyxlac or vMyxT5KO and activation of apoptotic enzymes was assessed by Western blotting. Neither cleavage of procaspase-3 to its active form nor processing of PARP, an enzyme responsible for the DNA fragmentation characteristic of apoptosis, was detectable in either cell line following infection

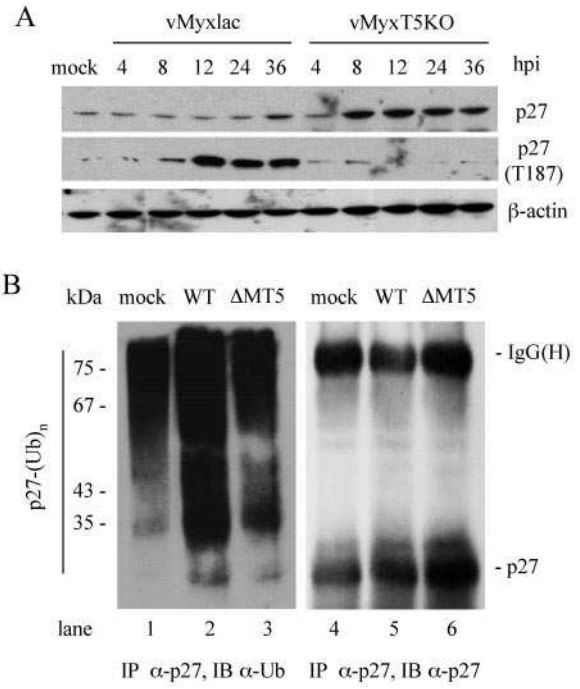

FIG. 5. Expression of M-T5 promotes ubiquitination and degradation of p27/Kip. A. Human 786-0 tumor cells were mock infected or infected with vMyxlac (WT) or vMyxT5KO (ΔMT5) at an MOI of 5, and p27 expression was determined by Western blotting at various times postinfection. Representative blots demonstrating levels of total p27 protein (p27), p27 specifically phosphorylated at threonine 187 (T187), and an actin loading control are shown. B. Ubiquitination of p27 was assessed in parallel cultures of 786-0 cells that were mock infected (lanes 1 and 4) or infected with vMyxlac (WT; lanes 2 and 5) or vMyxT5KO (ΔT5; lanes 3 and 6) as previously described. Cell lysates harvested at 17 h postinfection were subjected to immunoprecipitation (IP) using antibody specific for p27 (α-p27) and immunoblotting (IB) using antibody against Ub (α-Ub) (left panel) or p27 itself (right panel). The immunoglobulin G heavy chain [IgG(H)] is indicated.

with wild-type MV (Fig. 6A). Similar results were observed following infection of BGMK cells with KO virus. However, vMyxT5KO infection of 786-0 cells rapidly induced activation of caspase-3 and subsequent PARP cleavage, consistent with the increased p27 expression detected under the same conditions (Fig. 6A). To confirm that activation of enzymes associated with apoptosis correlated with progression to apoptosis, 786-0 and BGMK cells undergoing apoptosis were quantified by flow cytometry following Annexin V-PI staining at 24 hpi. As was observed by Western blotting, infection with vMyxlac was not associated with significant levels of apoptosis in either BGMK or 786-0 cells, although an approximately twofold increase in Annexin V-positive cells was detected in 786-0 cells (Fig. 6B). Again, M-T5 knockout virus infection of BGMK did not induce apoptosis, but a nearly 10-fold increase in apoptotic cells was observed in 786-0 cultures infected with vMyxT5KO compared to mock-infected cells (Fig. 6B). Similar results were also obtained when apoptosis was assessed by TUNEL assay to detect active DNA fragmentation. Infection with vMyxlac was not associated with apoptosis in either cell line, while vMyxT5KO infection of 786-0 cells, but not BGMK cells, re-

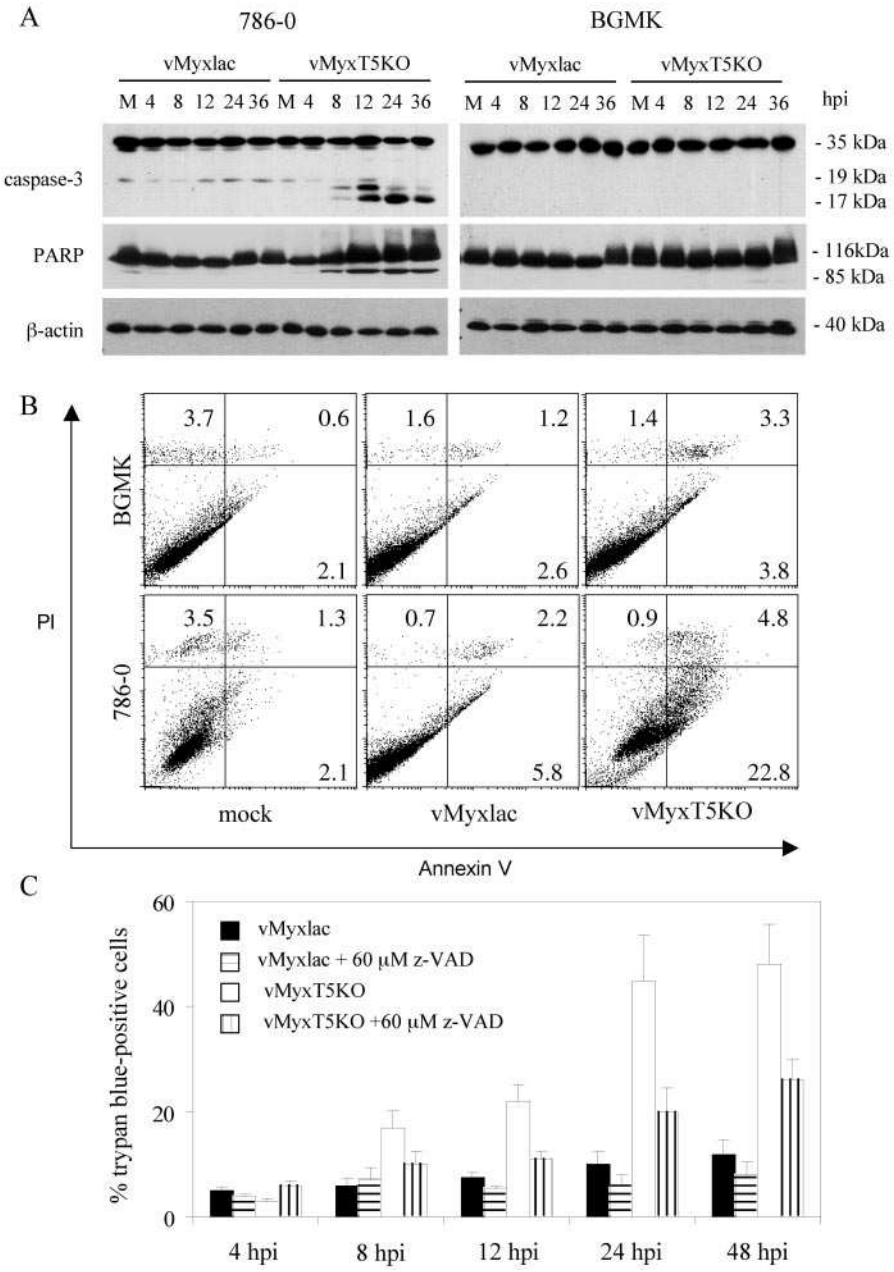

FIG. 6. Detection and characterization of cell death following infection. A. BGMK and 786-0 cells were mock infected (M) or infected with vMyxlac or vMyxT5KO at an MOI of 5, and caspase-3 and PARP expression levels were determined by Western blotting at various hours postinfection. Representative blots demonstrating processing of pro-caspase-3 (35 kDa) to its active forms (17 and 19 kDa) and cleavage of inactive PARP (116 kDa) to its active form (85 kDa) are shown. B. Apoptosis was detected in mock- and MV-infected cells at 24 hpi by Annexin V-PI staining and flow cytometry. Representative dot plots indicating cells stained with PI alone (upper left quadrant), Annexin V alone (lower right), or both (upper right) are shown. C. Cell death was detected by trypan blue exclusion assay in 786-0 cells infected with vMyxlac or vMyxT5KO at an MOI of 5 in the presence or absence of 60 μM z-VAD-FMK. Values are expressed as the mean percentage of trypan blue-positive cells (± standard deviation [SD]) from triplicate experiments.

sulted in a significant increase in TUNEL-positive cells compared to controls (data not shown).

We next assessed cell death using a less specific trypan blue exclusion assay. As with Annexin V staining, infection of 786-0 cells with vMyxT5KO induced significantly greater levels of cell death than that observed in parallel cultures infected with wild-type vMyxlac (Fig. 6C). However, more than twice as many dead or dying cells were detected using trypan blue than were detected in parallel experiments where Annexin V was used to detect cells undergoing apoptosis, suggesting that apoptosis was not the only mechanism of cell death induced by infection under nonpermissive conditions. This hypothesis was investigated using the pan-caspase inhibitor z-VAD-FMK (z-VAD) to inhibit caspase-mediated apoptotic cascades. Treat-

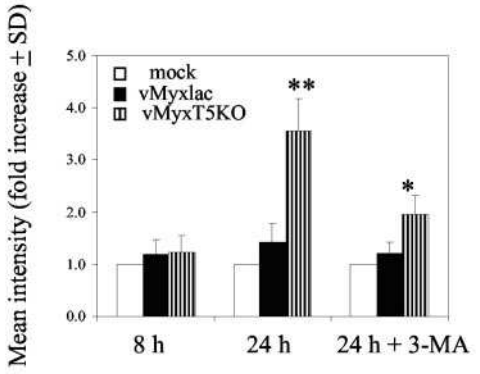

FIG. 7. Expression of M-T5 protects against autophagy. 786-0 cells were mock infected or infected with vMyxlac or vMyxT5KO at an MOI of 5 and stained with LysoTracker Red fluorescent dye at 8 and 24 hpi. Parallel cultures were preincubated with 10 μM of 3-MA for 3 h prior to infection. The intensity of fluorescent staining was detected by flow cytometry, and results are expressed relative to mock-infected cultures. Data from triplicate experiments are shown. *, $P < 0.05$; **, $P < 0.01$ (Student's t test).

ment of 786-0 cells with z-VAD only partially abrogated the cell death associated with vMyxT5KO infection, decreasing the number of trypan blue-positive cells by approximately 50% (Fig. 6C). In comparison, treatment of cells with z-VAD completely abrogated the lower level of cell death observed following infection with wild-type vMyxlac (Fig. 6C).

To explore this dichotomy, we investigated the potential that infected cells might also be succumbing to autophagy, another form of active programmed cell death that has been associated with cytotoxicity following stress-induced cell cycle arrest in tumor cells (19, 23, 57). Moreover, p27 accumulation has also been shown to induce autophagy in some tumor cell models in the absence of significant apoptosis (24, 57). Since autophagy is characterized by the formation of autophagic vacuoles that subsequently fuse with lysosomes to form low-pH autolysosomes (22), infected and uninfected cells were stained with the fluorescent dye Lysotracker Red, and the abundance of acidic vesicles was assessed by flow cytometry. As shown in Fig. 7, no significant differences were observed after 8 h between mock-infected cells and cells infected with either virus. However, at 24 hpi the mean fluorescence detected in cell cultures infected with vMyxT5KO was increased by 3.5-fold compared to mock-infected cells, indicating a greater abundance of lysosomal staining, while the mean fluorescence in vMyxlac-infected cells did not vary significantly from controls (Fig. 7). Moreover, the extent of this effect was greatly reduced when cells were infected in the presence of the known inhibitor of autophagy, 3-methyladenine (3-MA) (8). Although mean fluorescence remained greater in cultures infected with vMyxT5KO compared to the other two groups, treatment with 3-MA reduced this staining by approximately 50% (Fig. 7). These findings implicated M-T5 in the regulation of diverse cell death pathways induced following cell cycle arrest.

Expression of M-T5 decreases sensitivity to diverse stress stimuli. The above results investigated the role of M-T5 in suppressing the triggering of host responses to infection that culminate in activation of cell death pathways. To determine if

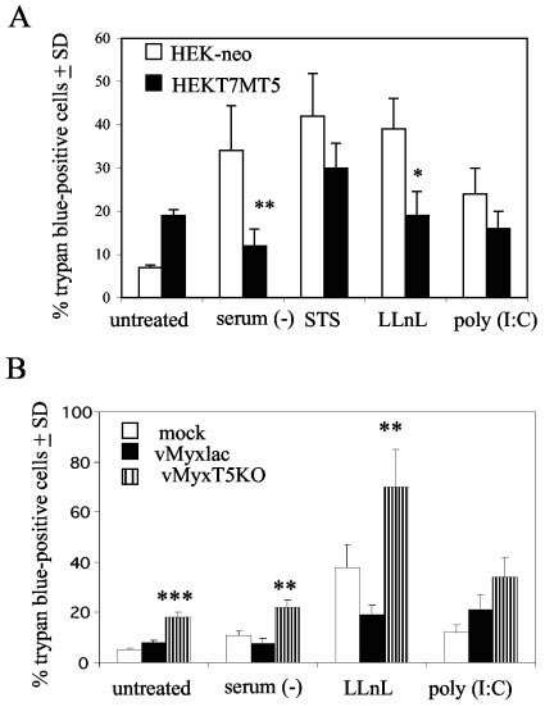

FIG. 8. Expression of M-T5 protects against stress stimuli other than infection. A. HEK293 cells were stably transfected with plasmid encoding T7-tagged M-T5 (HEKT7MT5) or the control neomycin cassette (HEK-neo), and cell death was assessed by trypan blue assay following various treatments. Treatments included serum deprivation for 24 h and incubation with staurosporine (STS, 50 nM) for 8 h, the proteasome inhibitor LLnL (10 μM) for 12 h, or dsRNA [poly(I:C), 20 μg/ml] for 12 h. Values represent the mean percentage of trypan blue-positive cells ± standard deviation (SD) from triplicate experiments. B. 786-0 cells were mock infected or infected with vMyxlac or vMyxT5KO at an MOI of 5, and cell death was assessed at 12 hpi by trypan blue assay following the treatments in panel A. *, $P < 0.05$; **, $P < 0.01$; ***, $P < 0.001$ (Student's t test).

this protective property extended to stress stimuli other than that of infection itself, HEK293 cells stably expressing T7-tagged M-T5 (HEKT7MT5) and a control cell stably transfected with the neomycin cassette (HEK-neo) were subjected to stimuli known to induce cell cycle arrest and cell death by apoptosis, autophagy, or both death pathways, and cell death was assessed by trypan blue exclusion. A modest difference in the basal level of cell death was observed between untreated HEKT7MT5 and HEK-neo cells (Fig. 8A). However, cell death was significantly decreased in cells expressing M-T5 compared to controls following serum deprivation for 24 h ($P < 0.001$) or treatment with the proteasome inhibitor LLnL for 12 h ($P < 0.01$) (Fig. 8A). Although decreased numbers of trypan blue-positive cells were also detectable in HEKT7MT5 cultures compared to controls following treatment with staurosporine (42.1 ± 5.8 cells versus 30.0 ± 9.8 cells) for 8 h or dsRNA (23.9 ± 6.0 cells versus 16.4 ± 3.9 cells) for 12 h, these decreases were not significantly different ($P = 0.07$ and $P = 0.23$, respectively) (Fig. 8A). Similar results were observed under infection conditions when 786-0 cells were mock infected or infected with vMyxlac or vMyxT5KO. Consistent with the results in Fig. 6, infection of untreated cells with

vMyxT5KO resulted in increased cell death compared to mock- and vMyxlac-infected cultures (Fig. 8B). In addition, like the HEK293 cells expressing M-T5, fewer trypan blue-positive cells were detected in vMyxlac-infected cultures subjected to serum deprivation or LLnL treatment compared to mock-infected cells (Fig. 8B). Moreover, cells infected with vMyxT5KO exhibited increased susceptibility to the toxic effects of these stimuli. Following serum deprivation or LLnL treatment, trypan blue-positive cells were increased approximately twofold in vMyxT5KO-infected cultures compared to mock-infected cells and 2.9-fold and 3.7-fold, respectively, compared to vMyxlac-infected cells (Fig. 8B). As with HEK293 cells, no significant differences were detected between cells infected with wild-type or KO virus following treatment with dsRNA. Thus, expression of M-T5 alone has the potential to reduce the toxic consequences of a variety of infections itself, as well as stress stimuli beyond those associated with infection. Whether these properties represent a functional consequence of the ability of M-T5 to interact with cul-1 and manipulate cell cycle progression remains a subject of ongoing investigation.

TABLE 1. Sensitivity of cell lines to proteasome inhibition and MV infection

Cell line[a]	Permissiveness to vMyxlac[b]	Permissiveness to vMyxT5KO	Sensitivity to LLnL[c]
BGMK	+	+	−
OMK	+	+	−
COS-7	+	+	−
HEK293	+	+	−
HOS	+	+	−
CAKI-1	+	+	−[d]
786-0	+	−	+
MCF-7	−	−	+
RK-13	+	+	−
RL-5	+	−	+

[a] BGMK, baby green monkey kidney; OMK, owl monkey kidney; COS-7, African geen monkey kidney; HEK293, human epithelial kidney; HOS, human osteosarcoma; RK-13, rabbit kidney; RL-5, rabbit lymphocyte.
[b] Cells were infected with the indicated virus, and replication was assessed by focus-forming assay.
[c] Cells were incubated with the proteasome inhibitor LLnL at a concentration of 50 μM for 12 h, and cell death was assessed by trypan blue exclusion.
[d] CAKI-1 cells began to exhibit sensitivity to LLnL at 24 h posttreatment.

DISCUSSION

MV M-T5 was initially identified as a poxvirus virulence factor, based on the observation that its deletion dramatically attenuated myxomatosis in susceptible rabbits, rendering the virus nonlethal (31). Moreover, loss of virulence was correlated with the complete cessation of host and virus protein synthesis in infected rabbit lymphocytes, thus leading to accelerated programmed cell death. More recently, wild-type MV was found to productively infect a diverse spectrum of human tumor cell lines, an ability that the deletion of both copies of the M-T5 gene either abrogated or reduced in the majority of the cell lines tested (45). In both human and leporine cells, loss of M-T5 was characterized by an abortive infection that resulted in a reduced spread of the M-T5 KO virus at a stage following entry of host cells. A potential explanation is provided by the results of the current study demonstrating that M-T5 has the ability to manipulate host cell cycle progression to promote transition of infected cells out of the G_0/G_1 phase and retention at the G_2/M checkpoint.

Physiological cell death responses are especially important for lymphocytes, given the need to establish and maintain an effective, yet self-limiting and nonautoreactive, repertoire of immune cells (48). Although cell death responses can be triggered in lymphocytes by a variety of stimuli, arrest at a postmitotic phase of the cell cycle is a common apoptotic initiator. Similarly, uncontrolled cell cycle progression is a hallmark of tumorigenesis, and the machinery responsible for apoptosis and cell cycle arrest is a common target for both pro- and antitumor mechanisms (26). Thus, control of the cell cycle to prevent replicative arrest and abort provides an attractive hypothesis to explain the role of M-T5 as a critical determinant of productive infection in both rabbit lymphocytes and transformed human cells. In contrast, cells which support productive infection by the M-T5 KO virus, such as BGMK cells (45), are highly resistant to diverse stimuli known to induce cell cycle arrest, including inhibitors of the Ub-proteasome degradation pathway. For example, we have observed that resistance to proteasome inhibitors correlates with permissiveness to the M-T5 KO virus in many cell lines other than BGMK cells (Table 1 and unpublished data). Taken together, these findings suggest that the ability to overcome growth arrest following infection is a fundamental determinant of the cell tropism of MV.

Our observation that M-T5 interacts with the E3 Ub ligase, cul-1, concurrent with an increase in the ubiquitination and degradation of p27/Kip-1 provides insight into the molecular mechanisms by which the protein contributes to MV pathogenesis. A member of the CIP/LIP family of CDK-I, which also includes p21/waf, p27/Kip is an important mediator of G_1 arrest in response to diverse stimuli, including virus infection, serum deprivation, interferons, and proinflammatory cytokines (44). Regulation of p27 occurs primarily at the posttranscriptional level, and regulated turnover of cyclins and CDK-I through selective degradation in the Ub-proteasome system represents the key mechanism for controlling progression through the cell cycle (37). Phosphorylation of p27 at Thr187 signals the subsequent degradation of p27, which was observed following expression of M-T5 in the current study, and has been shown to overcome G_1 arrest and promote entry into the S phase (50). In addition, degradation of p27 is dependent on the activity of SCFSkp2, a multicomponent ubiquitination complex that includes cul-1 (47). Thus, our results suggest that the interaction between M-T5 and cul-1 increases the turnover of p27 through increased proteolytic degradation. Moreover, this interaction appears to be specific for p27, because we have failed to see a similar increase in ubiquitination and degradation of other known substrates of cul-1, such as p21, p53, IκB-α, and E2F-1 (data not shown). However, the interaction between M-T5 and cul-1 is unlikely to be directly responsible for the increased phosphorylation of p27 detected in the presence of M-T5. A possible explanation may lie in our recent observation that M-T5 also can interact with the serine/threonine kinase, Akt, and that this interaction promotes activation of Akt kinase (unpublished data). Since p27 is a substrate of activated Akt (9), the increased phosphorylation and degradation of p27 may reflect concurrent enhancement of Akt and

cul-1 activity by M-T5. This possibility is currently being explored in greater detail.

Although the precise mechanism by which the M-T5–cul-1 interaction might enhance the ubiquitination activity of cul-1 has yet to be precisely ascertained, there are several plausible scenarios. Like p27, the activity of cullins is typically regulated by posttranslational events. For example, SCF is enhanced by the activity of several small Ub-like proteins, such as Nedd8, which covalently conjugate with cullins to increase the efficiency of their ligase activity. In fact, Nedd8 has been shown to promote the ubiquination of p27/Kip1 by SCFSkp2, thereby modulating cul-1 control of the G_1/G_0 and G_1/S transition (56). Thus, the interaction between M-T5 and cul-1 may directly enhance Ub ligase activity. Alternatively, the function of M-T5 may be more indirect. Substrate determination by SCFs is dependent on variable F-box proteins, such as Skp2, that recognize proteins targeted for ubiquitination based on specific phosphorylation profiles and bring them into close association with the catalytic subunits of the SCF through a second interaction with a linker protein, such as Skp1 (7). The presence of a putative C-terminal F-box-like motif within M-T5 also suggests the potential for the protein to enhance ubiquitination of target substrates by promoting their association with cul-1.

The presence of seven ANK repeat domains within M-T5 may also provide insight into its mechanism of action. The ANK repeat, a 33-residue domain named after the cytoskeletal protein ANK, was first identified in yeast cell cycle regulators and subsequently shown to be a feature of many proteins involved in regulation of the cell cycle, transcription, development, and cytoskeletal organization (29, 41). Moreover, ANK repeat-containing proteins are unusually abundant in chordopoxviruses and, like M-T5, they are often determinants of virus host range (43). For example, MV encodes three ANK repeat-containing proteins in addition to M-T5, the products of the M148R, M149R, and M150R open reading frames (2). Although the functions of M148R and M149R have yet to be elucidated, M150R has also been shown to be a MV host range determinant that is predicted to disrupt host inflammatory responses to infection by regulating activation of nuclear factor κB (3). Of note, M150R, like M-T5, was found to localize to the nucleus despite the lack of a traditional nuclear localization sequence, a property that mapped to one of its ANK repeats (3). Although the diversity exhibited by ANK proteins makes it unlikely that they share a common function, the role of the ANK domain as a protein-protein interaction motif is well established. Therefore, it is feasible that many of the properties of M-T5 can also be attributed to the ANK domains it encodes.

The role of M-T5 as a putative cell cycle regulator is further supported by earlier studies that proposed a connection between manipulation of the cell cycle and the virulence of leporipoxviruses. Consistent with our findings using MV, infection with the closely related virulent MRV was also found to promote accumulation of host cells in G_2/M (51). In contrast, the apathogenic SFV did not produce this effect and instead exhibited a profile that more closely resembled the M-T5 knockout (51). MRV is a chimeric virus that arose following spontaneous recombination between MV and SFV (49). One consequence of these events is that both copies of the MRV T5 genes represent an in-frame fusion of the M-T5 gene from MV and S-T5 of SFV. As a result, the T5 gene product of MRV encodes the C terminus of MV M-T5 (amino acids 232 to 483) and the N terminus of SFV S-T5. Thus, MV and MRV, which possess similar abilities to manipulate the cell cycle upon infection, share common sequences within their T5 genes that encode an F-box domain and at least two ANK repeats.

Infection by virtually all viruses directly impacts on the cell cycle, either inducing a replicative block at a specific transitional phase or overcoming host cell-induced arrest, which is commonly a precursor to the apoptosis and clearance of infected cells. The genomes of poxviruses, like other large DNA viruses, encode numerous proteins with the specific function of modulating the host immune responses to infection and creating an environment conducive to viral replication and spread (43). Moreover, the vast majority of these strategies share the common goal of regulating events involving the concerted activity of diverse death pathways. Our results indicate M-T5 can regulate how cell cycle arrest triggers programmed cell death pathways that include elements of both apoptosis and autophagy. The role of p27/Kip in both pathways has been established, emphasizing how regulation of the cell cycle has important implications for the pathogenesis of even complex DNA viruses that replicate independent of the host nuclear machinery, such as poxviruses. Further study of these events has the potential to contribute greatly to our understanding of the selective pressures that drive the coevolution of virus and host.

ACKNOWLEDGMENTS

We thank Y. Xiong (UNC) for helpful discussions concerning cullin function and Doris Hall for assistance with the manuscript.

This work is supported by the CIHR of Canada. G.M. holds a Canada Research Chair in Molecular Virology, and J.B.J. held a CIHR Fellowship award.

REFERENCES

1. **Boyer, S. N., D. E. Wazer, and V. Band.** 1996. E7 protein of human papilloma virus-16 induces degradation of retinoblastoma protein through the ubiquitin-proteasome pathway. Cancer Res **56:**4620–4624.
2. **Cameron, C., S. Hota-Mitchell, L. Chen, J. Barrett, J. X. Cao, C. Macaulay, D. Willer, D. Evans, and G. McFadden.** 1999. The complete DNA sequence of myxoma virus. Virology **264:**298–318.
3. **Camus-Bouclainville, C., L. Fiette, S. Bouchiha, B. Pignolet, D. Counor, C. Filipe, J. Gelfi, and F. Messud-Petit.** 2004. A virulence factor of myxoma virus colocalizes with NF-κB in the nucleus and interferes with inflammation. J. Virol. **78:**2510–2516.
4. **Cardozo, T., and M. Pagano.** 2004. The SCF ubiquitin ligase: insights into a molecular machine. Nat. Rev. Mol. Cell Biol. **5:**739–751.
5. **Coscoy, L., D. J. Sanchez, and D. Ganem.** 2001. A novel class of herpesvirus-encoded membrane-bound E3 ubiquitin ligases regulates endocytosis of proteins involved in immune recognition. J. Cell Biol. **155:**1265–1273.
6. **De Bolle, L., S. Hatse, E. Verbeken, E. De Clercq, and L. Naesens.** 2004. Human herpesvirus 6 infection arrests cord blood mononuclear cells in G_2 phase of the cell cycle. FEBS Lett. **560:**25–29.
7. **Deshaies, R. J.** 1999. SCF and Cullin/Ring H2-based ubiquitin ligases. Annu. Rev. Cell Dev. Biol. **15:**435–467.
8. **Eskelinen, E. L., A. R. Prescott, J. Cooper, S. M. Brachmann, L. Wang, X. Tang, J. M. Backer, and J. M. Lucocq.** 2002. Inhibition of autophagy in mitotic animal cells. Traffic **3:**878–893.
9. **Fujita, N., S. Sato, K. Katayama, and T. Tsuruo.** 2002. Akt-dependent phosphorylation of p27Kip1 promotes binding to 14-3-3 and cytoplasmic localization. J. Biol. Chem. **277:**28706–28713.
10. **Gemeniano, M. C., E. T. Sawai, and E. E. Sparger.** 2004. Feline immunodeficiency virus Orf-A localizes to the nucleus and induces cell cycle arrest. Virology **325:**167–174.
11. **Guerin, J. L., J. Gelfi, S. Boullier, M. Delverdier, F. A. Bellanger, S. Bertagnoli, I. Drexler, G. Sutter, and F. Messud-Petit.** 2002. Myxoma virus leukemia-associated protein is responsible for major histocompatibility complex class I and Fas-CD95 down-regulation and defines scrapins, a new group of surface cellular receptor abductor proteins. J. Virol. **76:**2912–2923.
12. **Huang, J., Q. Huang, X. Zhou, M. M. Shen, A. Yen, S. X. Yu, G. Dong, K. Qu,**

P. Huang, E. M. Anderson, S. Daniel-Issakani, R. M. Buller, D. G. Payan, and H. H. Lu. 2004. The poxvirus p28 virulence factor is an E3 ubiquitin ligase. J. Biol. Chem. **279:**54110–54116.
13. **Izumiya, Y., S. F. Lin, T. Ellison, L. Y. Chen, C. Izumiya, P. Luciw, and H. J. Kung.** 2003. Kaposi's sarcoma-associated herpesvirus K-bZIP is a coregulator of K-Rta: physical association and promoter-dependent transcriptional repression. J. Virol. **77:**1441–1451.
14. **Johnston, J. B., J. W. Barrett, W. Chang, C. S. Chung, W. Zeng, J. Masters, M. Mann, F. Wang, J. Cao, and G. McFadden.** 2003. Role of the serine-threonine kinase PAK-1 in myxoma virus replication. J. Virol. **77:**5877–5888.
15. **Johnston, J. B., S. H. Nazarian, R. Natale, and G. McFadden.** 2005. Myxoma virus infection of primary human fibroblasts varies with cellular age and is regulated by host interferon responses. Virology **332:**235–248.
16. **Jowett, J. B., V. Planelles, B. Poon, N. P. Shah, M. L. Chen, and I. S. Chen.** 1995. The human immunodeficiency virus type 1 vpr gene arrests infected T cells in the G_2 + M phase of the cell cycle. J. Virol. **69:**6304–6313.
17. **Kalejta, R. F., J. T. Bechtel, and T. Shenk.** 2003. Human cytomegalovirus pp71 stimulates cell cycle progression by inducing the proteasome-dependent degradation of the retinoblastoma family of tumor suppressors. Mol. Cell. Biol. **23:**1885–1895.
18. **Kalejta, R. F., and T. Shenk.** 2003. The human cytomegalovirus UL82 gene product (pp71) accelerates progression through the G_1 phase of the cell cycle. J. Virol. **77:**3451–3459.
19. **Kanzawa, T., Y. Kondo, H. Ito, S. Kondo, and I. Germano.** 2003. Induction of autophagic cell death in malignant glioma cells by arsenic trioxide. Cancer Res **63:**2103–2108.
20. **Katner, A. L., P. Gootam, Q. B. Hoang, J. R. Gnarra, and W. Rayford.** 2002. A recombinant adenovirus expressing p7(Kip1) induces cell cycle arrest and apoptosis in human 786-0 renal carcinoma cells. J. Urol. **168:**766–773.
21. **Katner, A. L., Q. B. Hoang, P. Gootam, E. Jaruga, Q. Ma, J. Gnarra, and W. Rayford.** 2002. Induction of cell cycle arrest and apoptosis in human prostate carcinoma cells by a recombinant adenovirus expressing p27(Kip1). Prostate **53:**77–87.
22. **Kirkegaard, K., M. P. Taylor, and W. T. Jackson.** 2004. Cellular autophagy: surrender, avoidance and subversion by microorganisms. Nat. Rev. Microbiol. **2:**301–314.
23. **Komata, T., T. Kanzawa, T. Nashimoto, H. Aoki, S. Endo, M. Nameta, H. Takahashi, T. Yamamoto, S. Kondo, and R. Tanaka.** 2004. Mild heat shock induces autophagic growth arrest, but not apoptosis in U251-MG and U87-MG human malignant glioma cells. J. Neurooncol. **68:**101–111.
24. **Komata, T., T. Kanzawa, H. Takeuchi, I. M. Germano, M. Schreiber, Y. Kondo, and S. Kondo.** 2003. Antitumour effect of cyclin-dependent kinase inhibitors ($p16^{INK4A}$, $p18^{INK4C}$, $p19^{INK4D}$, $p21^{WAF1/CIP1}$ and $p27^{KIP1}$) on malignant glioma cells. Br. J. Cancer **88:**1277–1280.
25. **Li, J., X. K. Yang, X. X. Yu, M. L. Ge, W. L. Wang, J. Zhang, and Y. D. Hou.** 2000. Overexpression of $p27^{KIP1}$ induced cell cycle arrest in G_1 phase and subsequent apoptosis in HCC-9204 cell line. World J. Gastroenterol. **6:**513–521.
26. **Lowe, S. W., E. Cepero, and G. Evan.** 2004. Intrinsic tumour suppression. Nature **432:**307–315.
27. **Mansouri, M., E. Bartee, K. Gouveia, B. T. Hovey Nerenberg, J. Barrett, L. Thomas, G. Thomas, G. McFadden, and K. Fruh.** 2003. The PHD/LAP-domain protein M153R of myxomavirus is a ubiquitin ligase that induces the rapid internalization and lysosomal destruction of CD4. J. Virol. **77:**1427–1440.
28. **Mitsuhashi, T., Y. Aoki, Y. Z. Eksioglu, T. Takahashi, P. G. Bhide, S. A. Reeves, and V. S. Caviness, Jr.** 2001. Overexpression of p27Kip1 lengthens the G_1 phase in a mouse model that targets inducible gene expression to central nervous system progenitor cells. Proc. Natl. Acad. Sci. USA **98:**6435–6440.
29. **Mosavi, L. K., T. J. Cammett, D. C. Desrosiers, and Z. Y. Peng.** 2004. The ankyrin repeat as molecular architecture for protein recognition. Protein Sci. **13:**1435–1448.
30. **Moss, B.** 2001. *Poxviridae*: the virus and their replication, p. 2849–2883. *In* D. M. Knipe and P. M. Howley (ed.), Fields virology, 4th ed., vol. 2. Lippincott Williams and Wilkins, Philadelphia, Pa.
31. **Mossman, K., S. F. Lee, M. Barry, L. Boshkov, and G. McFadden.** 1996. Disruption of M-T5, a novel myxoma virus gene member of poxvirus host range superfamily, results in dramatic attenuation of myxomatosis in infected European rabbits. J. Virol. **70:**4394–4410.
32. **Murray, A. W.** 2004. Recycling the cell cycle: cyclins revisited. Cell **116:**221–234.
33. **Nakajima, T., M. Masuda-Murata, E. Hara, and K. Oda.** 1987. Induction of cell cycle progression by adenovirus E1A gene 13S and 12S mRNA products in quiescent rat cells. Mol. Cell. Biol. **7:**3846–3852.
34. **Nakayama, K. I., S. Hatakeyama, and K. Nakayama.** 2001. Regulation of the cell cycle at the G_1-S transition by proteolysis of cyclin E and p27Kip1. Biochem. Biophys. Res. Commun. **282:**853–860.
35. **Nerenberg, B. T., J. Taylor, E. Bartee, K. Gouveia, M. Barry, and K. Fruh.** 2005. The poxviral RING protein p28 is a ubiquitin ligase that targets ubiquitin to viral replication factories. J. Virol. **79:**597–601.
36. **Opgenorth, A., K. Graham, N. Nation, D. Strayer, and G. McFadden.** 1992. Deletion analysis of two tandemly arranged virulence genes in myxoma virus, M11L and myxoma growth factor. J. Virol. **66:**4720–4731.
37. **Pagano, M., S. W. Tam, A. M. Theodoras, P. Beer-Romero, G. Del Sal, V. Chau, P. R. Yew, G. F. Draetta, and M. Rolfe.** 1995. Role of the ubiquitin-proteasome pathway in regulating abundance of the cyclin-dependent kinase inhibitor p27. Science **269:**682–685.
38. **Pickart, C. M., and R. E. Cohen.** 2004. Proteasomes and their kin: proteases in the machine age. Nat. Rev. Mol. Cell Biol. **5:**177–187.
39. **Pickart, C. M., and M. J. Eddins.** 2004. Ubiquitin: structures, functions, mechanisms. Biochim. Biophys. Acta **1695:**55–72.
40. **Querido, E., P. Blanchette, Q. Yan, T. Kamura, M. Morrison, D. Boivin, W. G. Kaelin, R. C. Conaway, J. W. Conaway, and P. E. Branton.** 2001. Degradation of p53 by adenovirus E4orf6 and E1B55K proteins occurs via a novel mechanism involving a Cullin-containing complex. Genes Dev. **15:**3104–3117.
41. **Rubtsov, A. M., and O. D. Lopina.** 2000. Ankyrins. FEBS Lett. **482:**1–5.
42. **Seeger, M., K. Ferrell, R. Frank, and W. Dubiel.** 1997. HIV-1 tat inhibits the 20 S proteasome and its 11 S regulator-mediated activation. J. Biol. Chem. **272:**8145–8148.
43. **Seet, B. T., J. B. Johnston, C. R. Brunetti, J. W. Barrett, H. Everett, C. Cameron, J. Sypula, S. H. Nazarian, A. Lucas, and G. McFadden.** 2003. Poxviruses and immune evasion. Annu. Rev. Immunol. **21:**377–423.
44. **Sgambato, A., A. Cittadini, B. Faraglia, and I. B. Weinstein.** 2000. Multiple functions of $p27^{Kip1}$ and its alterations in tumor cells: a review. J. Cell Physiol. **183:**18–27.
45. **Sypula, J., F. Wang, Y. Ma, J. Bell, and G. McFadden.** 2004. Myxoma virus tropism in human tumor cells. Gene Ther. Mol. Biol. **8:**103–114.
46. **Thomas, M., D. Pim, and L. Banks.** 1999. The role of the E6-p53 interaction in the molecular pathogenesis of HPV. Oncogene **18:**7690–7700.
47. **Tsvetkov, L. M., K. H. Yeh, S. J. Lee, H. Sun, and H. Zhang.** 1999. $p27^{Kip1}$ ubiquitination and degradation is regulated by the SCF^{Skp2} complex through phosphorylated Thr187 in p27. Curr. Biol. **9:**661–664.
48. **Ucker, D. S., L. D. Hebshi, J. F. Blomquist, and B. E. Torbett.** 1994. Physiological T-cell death: susceptibility is modulated by activation, aging, and transformation, but the mechanism is constant. Immunol. Rev. **142:**273–299.
49. **Upton, C., J. L. Macen, R. A. Maranchuk, A. M. DeLange, and G. McFadden.** 1988. Tumorigenic poxviruses: fine analysis of the recombination junctions in malignant rabbit fibroma virus, a recombinant between Shope fibroma virus and myxoma virus. Virology **166:**229–239.
50. **Vlach, J., S. Hennecke, and B. Amati.** 1997. Phosphorylation-dependent degradation of the cyclin-dependent kinase inhibitor p27. EMBO J. **16:**5334–5344.
51. **Wali, A., and D. S. Strayer.** 1999. Comparative effects of virulent and avirulent poxviruses on cell cycle progression. Exp. Mol. Pathol. **66:**31–38.
52. **Wali, A., and D. S. Strayer.** 1999. Infection with vaccinia virus alters regulation of cell cycle progression. DNA Cell Biol. **18:**837–843.
53. **Wang, F., Y. Ma, J. W. Barrett, X. Gao, J. Loh, E. Barton, H. W. Virgin, and G. McFadden.** 2004. Disruption of Erk-dependent type I interferon induction breaks the myxoma virus species barrier. Nat. Immunol. **5:**1266–1274.
54. **Wang, G., J. W. Barrett, S. H. Nazarian, H. Everett, X. Gao, C. Bleackley, K. Colwill, M. F. Moran, and G. McFadden.** 2004. Myxoma virus M11L prevents apoptosis through constitutive interaction with Bak. J. Virol. **78:**7097–7111.
55. **Wang, X., M. Gorospe, Y. Huang, and N. J. Holbrook.** 1997. $p27^{Kip1}$ overexpression causes apoptotic death of mammalian cells. Oncogene **15:**2991–2997.
56. **Wu, K., A. Chen, and Z. Q. Pan.** 2000. Conjugation of Nedd8 to CUL1 enhances the ability of the ROC1-CUL1 complex to promote ubiquitin polymerization. J. Biol. Chem. **275:**32317–32324.
57. **Yao, K. C., T. Komata, Y. Kondo, T. Kanzawa, S. Kondo, and I. M. Germano.** 2003. Molecular response of human glioblastoma multiforme cells to ionizing radiation: cell cycle arrest, modulation of the expression of cyclin-dependent kinase inhibitors, and autophagy. J. Neurosurg. **98:**378–384.